

OAK RIDGE
NATIONAL
LABORATORY

MARTIN MARIETTA

Second Stability Studies in the ATF Torsatron

M. Murakami
S. A. Carreras
J. H. Harris

F. S. B. Anderson	A. C. England	V. E. Lynch
G. L. Bell	J. C. Glowienka	M. M. Menon
J. D. Bell	L. D. Horton	R. N. Morris
T. S. Bigelow	H. C. Howe	G. H. Neilson
R. J. Colchin	R. C. Isler	V. K. Paré
E. C. Crume	H. Kaneko	D. A. Pasmussen
N. Dominguez	R. Kindsfather	J. B. Wilgen
J. L. Dunlap	J. N. Leboeuf	W. R. Wing

OAK RIDGE NATIONAL LABORATORY
 CENTRAL RESEARCH LIBRARY
 CIRCULATION SECTION
 4th floor, room 112
LIBRARY LOAN COPY
 DO NOT TRANSFER TO ANOTHER PERSON
 If you wish someone else to see this
 report, send to same with report and
 the library will arrange a loan.

Fusion Energy Division

SECOND STABILITY STUDIES IN THE ATF TORSATRON

M. Murakami	N. Dominguez	J. N. Leboeuf
B. A. Carreras	J. L. Dunlap	V. E. Lynch [†]
J. H. Harris	A. C. England	M. M. Menon
F. S. B. Anderson*	J. C. Glowienka	R. N. Morris [†]
G. L. Bell [†]	L. D. Horton	G. H. Neilson
J. D. Bell [†]	H. C. Howe	V. K. Paré
T. S. Bigelow	R. C. Isler	D. A. Rasmussen
R. J. Colchin	H. Kaneko**	J. B. Wilgen
E. C. Crume	R. Kindsfather	W. R. Wing

This paper was prepared for presentation at the 16th European Conference on Controlled Fusion and Plasma Physics, Venice, Italy, March 13-17, 1989, and will be published in the proceedings.

*University of Wisconsin, Madison.

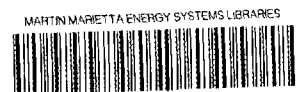
[†]Auburn University, Auburn, Alabama.

[‡]Computing and Telecommunications Division, Martin Marietta Energy Systems, Inc.

**Kyoto University, Uji, Kyoto, Japan.

Date Published—March 1989

Prepared by the
OAK RIDGE NATIONAL LABORATORY
Oak Ridge, Tennessee 37831
operated by
MARTIN MARIETTA ENERGY SYSTEMS, INC.
for the
U.S. DEPARTMENT OF ENERGY
under contract DE-AC05-84OR21400



3 4456 0290639 0

CONTENTS

ABSTRACT	v
INTRODUCTION	1
EXPERIMENTAL CONDITIONS	1
MHD STABILITY ANALYSIS	4
FLUCTUATION MEASUREMENTS	5
EFFECTS ON CONFINEMENT	7
ACKNOWLEDGMENT	9
REFERENCES	10

ABSTRACT

The Advanced Toroidal Facility (ATF) is a stellarator designed to have stable access to the second stability (or beta self-stabilization) regime, which should be reached when the deepening magnetic well, caused by an increase in the Shafranov shift with increasing beta, stabilizes pressure-driven (interchange) instabilities. During its initial operating phase, ATF was operated with magnetic islands that resulted from field errors (which have since been corrected). The resulting peaked pressure profiles actually facilitated access to the second stability regime. The highest central beta ($\approx 3\%$) achieved in the experiment is well above theoretical values ($\leq 1.3\%$) for the transition to the second stability regime. Measured magnetic fluctuations decrease with increasing beta, and the pressure profiles broaden. This behavior is consistent with theoretical predictions for beta self-stabilization of resistive interchange modes.

INTRODUCTION

The Advanced Toroidal Facility (ATF) is a stellarator designed to have direct access to the second stability (beta self-stabilization) regime [1]. This regime should be reached when deepening of the magnetic well, caused by increased Shafranov shift with increasing beta, stabilizes pressure-driven (interchange) instabilities. In the initial operating phase, ATF was operated with magnetic islands due to field errors [2,3] (which have since been corrected). The resulting reduction in effective plasma radius and edge transform caused larger Shafranov shift and improved stability properties for a given value of beta. Thus, the field errors actually facilitated access to the second stability regime. We discuss (1) experimental conditions for these studies, (2) the theoretical threshold for the second stability regime, (3) magnetic fluctuation measurements and predicted beta self-stabilization, and (4) confinement behavior.

EXPERIMENTAL CONDITIONS

ATF is a continuous-coil, $\ell = 2$, 12-field-period torsatron with major radius $R_0 = 2.10$ m, average minor radius $\bar{a} = 0.27$ m, magnetic field on axis $B_0 < 2$ T, and rotational transform $0.3 < \iota(r) < 1.0$. It has a 0.2-MW, 53-GHz electron cyclotron heating (ECH) system for currentless target plasma production and a 2-MW, 40-keV, 0.3-s co-plus-counter tangential neutral beam injection (NBI) system for high-power bulk heating. Experiments began in January 1988. Field mapping [3] in May 1988 with an electron-beam/fluorescent screen technique revealed 6-cm-wide magnetic islands at the $\iota = 1/2$ surface and smaller ones at other rational surfaces. These islands were later found to result from the design of the current feeds to the helical and outer vertical field coils. Corrective measures were taken, and electron-beam experiments to confirm the correction are now in progress.

Wall conditioning [4] (with electron cyclotron resonance and glow discharge cleaning combined with baking the vessel up to 150°C) was effective in producing ECH plasmas lasting for up to 1 s with no radiative collapse. However, neutral-beam-heated discharges were more sensitive to low- Z impurity radiation (particularly oxygen and carbon) [5] and thermally collapsed before the beam pulses ended [6]. Partial-coverage (<30%) chromium gettering proved beneficial in extending the duration of the neutral beam pulse and substantially increased the achievable plasma density and stored energy.

Figure 1 shows the time evolution of several parameters for a typical H^+ discharge with balanced beam injection of 1.4 MW total H^0 power into the gettered torus. The stored energy, measured with a diamagnetic loop, reached $W_{\text{dia}} = 7$ kJ with $\bar{n}_e = 2.5 \times 10^{19} \text{ m}^{-3}$, $n_{e0} \simeq 5 \times 10^{19} \text{ m}^{-3}$, $T_{e0} \simeq 0.26$ eV. This value of W_{dia} at $B_0 = 0.95$ T corresponds to volume-average beta $\langle \beta \rangle = 0.5\%$. For this case, the central beta is $\beta_0 = 2.8\text{--}3.2\%$, depending on diamagnetic or equilibrium weighting of small anisotropic beam contributions. Figure 2(a) shows the electron temperature profile measured with Thomson scattering at $R_0 = 2.10$ m and then mapped into the radial flux coordinate ρ in the finite-beta equilibrium geometry. The equilibrium was calculated by the VMEC code with the self-consistent pressure profile shown in Fig. 2(b). Such narrow T_e profiles were observed in both ECH and NBI phases and are probably due to the islands at the $\iota = 1/2$ surface, which effectively reduce the plasma radius to $r_p \simeq 0.6\bar{a}$. The narrow pressure profile resulted in a large outward Shafranov shift ($\delta = 0.11 \text{ m} \simeq 0.4\bar{a}$).

The field errors may also affect the sensitivity of global confinement parameters (W_{dia} and \bar{n}_e) to the vacuum axis shift [2]. The optimal position (at least at low

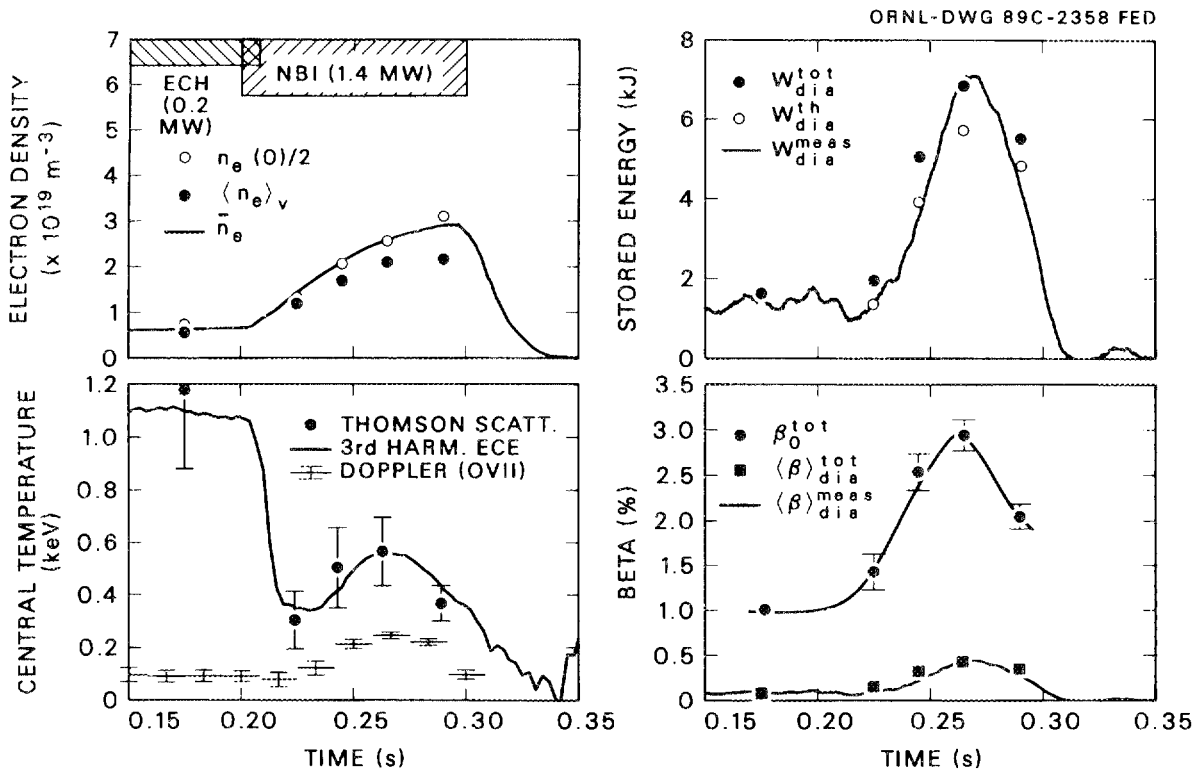


Fig. 1. Characteristics of a typical discharge.

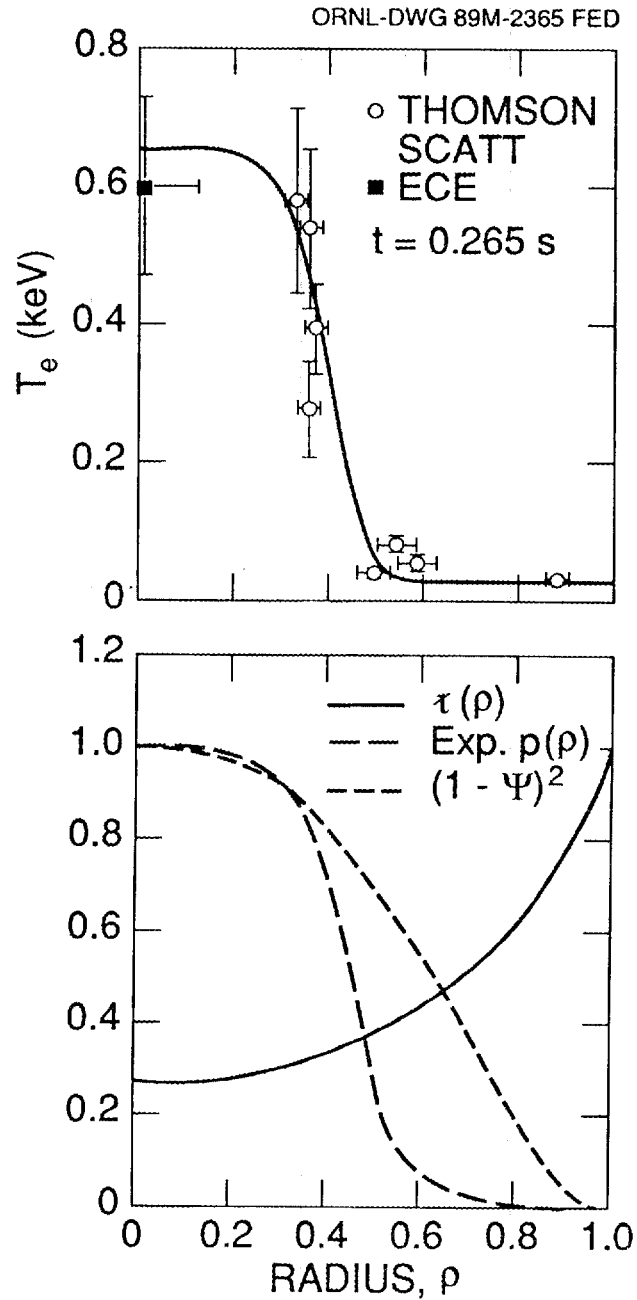


Fig. 2. Radial profiles of electron temperature (top) and rotational transform and total pressure (bottom).

beta) was found to be with the vacuum magnetic axis shifted in ~ 5 cm from the standard configuration, and all of the experiments discussed here were conducted with this inward shift, so that $R_0 = 2.05$ m. The inward shift minimized the $t = 1/2$ island width in the vacuum field; significantly larger inward shifts spoiled vacuum stability properties by increasing the destabilizing magnetic hill. As discussed below,

the vacuum configuration with a slight magnetic hill at $R_0 = 2.05$ m, combined with large Shafranov shift, made it possible to pass through a narrow, weakly unstable regime as beta increased.

MHD STABILITY ANALYSIS

Ideal MHD stability was examined [7] using the Mercier stability criterion ($D_m > 0$) for the equilibrium sequence with the “experimental” pressure profiles. Although the criterion is an asymptotic limit for high- n modes, the stability boundaries for low- n modes generally agree well with those for the Mercier modes. At a given radius (e.g., $\rho = 0.52$, where a large ∇p exists), D_m shows weak instability in the unstable regime. The transition to second stability occurs at relatively low β_0 ($= 1.3\%$), above which D_m increases sharply, reflecting a strong beta self-stabilization effect. Complete stability at all radii is attained at $\beta_0 > 1.3\%$ for zero-current equilibria (as shown in Fig. 3) and at $\beta_0 > 1.6\%$ for flux-conserving

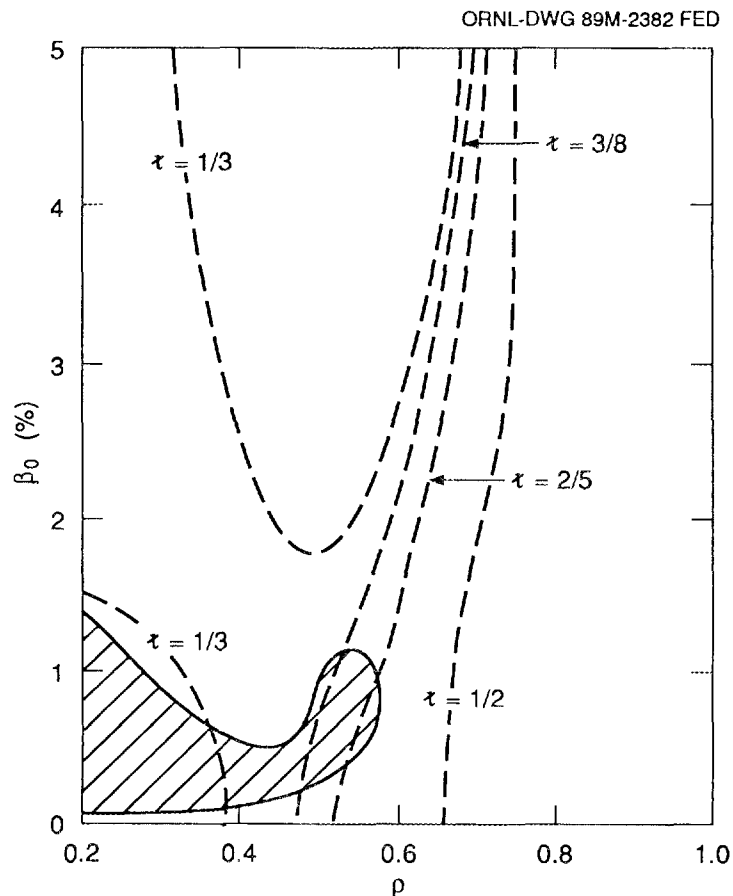


Fig. 3. Calculated ideal stability boundaries and rotational transform contour. The shaded area is the unstable region.

equilibria. The values achieved in the experiment (β_0 up to 3%) are well above these theoretically predicted thresholds.

Finite-resistivity plasmas exhibit fluctuations even in the second stability regime, which is an ideal MHD concept. The relevant instabilities are resistive interchange (∇p -driven) modes. Theoretically, beta self-stabilization, which stabilizes the ideal modes, also reduces the saturation amplitude of the resistive modes as beta increases [8]. In this sense, the resistive modes serve a probe to detect access to the second stability regime. These modes are primarily electrostatic (\tilde{n} and $\tilde{\phi}$), and thus magnetic components (\tilde{B}) are expected to be small. The dependence of magnetic fluctuation on β_0 , calculated from the saturation level of $\tilde{\phi}$, is shown in Fig. 4. Fluctuations caused by resistive interchange modes do not disappear in the second stability regime (particularly near the plasma edge), but show the effect of beta self-stabilization in the region where ∇p is large ($\rho = 0.6$), as shown in Fig. 4.

FLUCTUATION MEASUREMENTS

Initial fluctuation measurements [9] on ATF were made with a soft X-ray diode array (on loan from the Heliotron-E group) viewing the central portion of the plasma

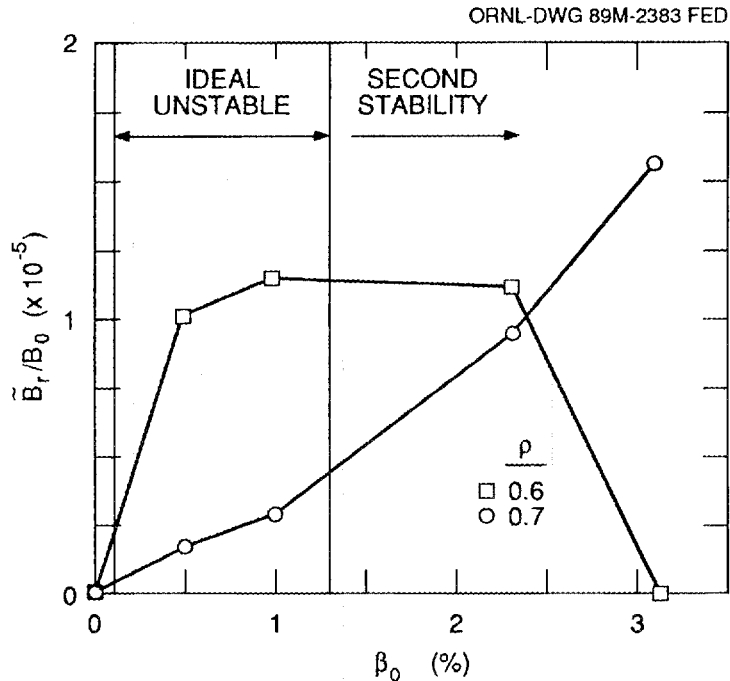


Fig. 4. Theoretically predicted levels of magnetic fluctuations versus central beta.

($\rho \leq 0.5$) and with Mirnov coils (\tilde{B}_θ) located ~ 30 cm outside the plasma. The soft X-ray signals show no evidence of gross instabilities such as sawteeth or disruptions.

Spectral analysis of \tilde{B}_θ data from Mirnov coils separated in toroidal angle by $\Delta\phi = 30^\circ, 150^\circ,$ and 180° reveals coherent fluctuations (frequency-resolved coherence function $\gamma > 0.7$) in the frequency range 8–40 kHz with amplitudes $\sim 10^{-3}$ G. The relative phase shifts of the signals are predominantly consistent with $n = 1$ toroidal mode symmetry, but some evidence of $n = 3$ components is seen for $\Delta\phi = 30^\circ$. No corresponding coherent activity is seen in the soft X-ray signals. It is difficult to determine the poloidal mode number (m) spectrum at present, because only two poloidally spaced Mirnov coils ($\Delta\theta = 150^\circ$) were available for these experiments; the non-circular flux surface geometry of ATF further complicates the determination of mode numbers. The available spectral data indicate that the fluctuations contain at least two poloidal harmonics, one of which can most simply be interpreted as $m = 2$.

The dependence of the \tilde{B}_θ amplitudes of the $n = 1$ mode (integrated over 8–40 kHz) on plasma pressure, shown in Fig. 5, suggests (1) a pressure threshold for the fluctuations at $\beta_0 < 1\%$ and (2) saturation and possible reduction of $\tilde{B}_\theta(n = 1)$

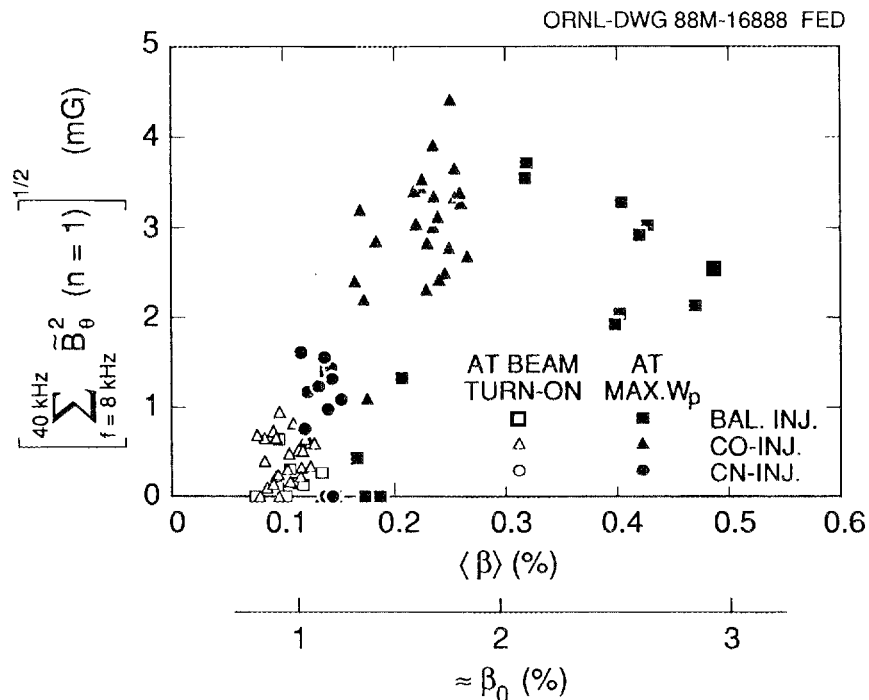


Fig. 5. Observed $n = 1$ magnetic fluctuation amplitudes versus volume-averaged beta.

as β_0 exceeds 1.5%. Additional trend analysis shows no obvious correlation with beam configuration or plasma current. The amplitude and overall behavior of the fluctuations are strongly reminiscent of the theoretical predictions for pressure-driven instabilities in ATF.

EFFECTS ON CONFINEMENT

Figure 6 shows a profile “broadness” parameter (and corresponding approximate $\langle\beta\rangle/\beta_0$ based on a few profile-analyzed cases) as a function of $\langle\beta\rangle$ for the fluctuation shot database. The pressure profiles broaden rapidly as beta increases; this effect saturates for $\beta_0 \geq 1.5\%$. Although many mechanisms could be responsible for such broadening (e.g., change of heating deposition profile), this behavior is *consistent* with growth of the plasma volume and reduced fluctuations (or anomalous transport losses) as the region of magnetic well expands with increasing beta. Figure 7 shows global energy confinement time (τ_E^*) versus $\langle\beta\rangle$ for data taken at maximum W_{dia} (i.e., not including data at beam turn-on) in the fluctuation database, overlaid with data from a wider “sequence” (averaged over a large number of shots) database. The improvement at high beta is due to increasing \bar{n}_e . Figure 8 shows the dependence of $\langle\beta\rangle$ on density for the sequence database. For a given injection power and state of cleanliness, $\langle\beta\rangle$ increases roughly linearly with \bar{n}_e , then saturates and decreases.

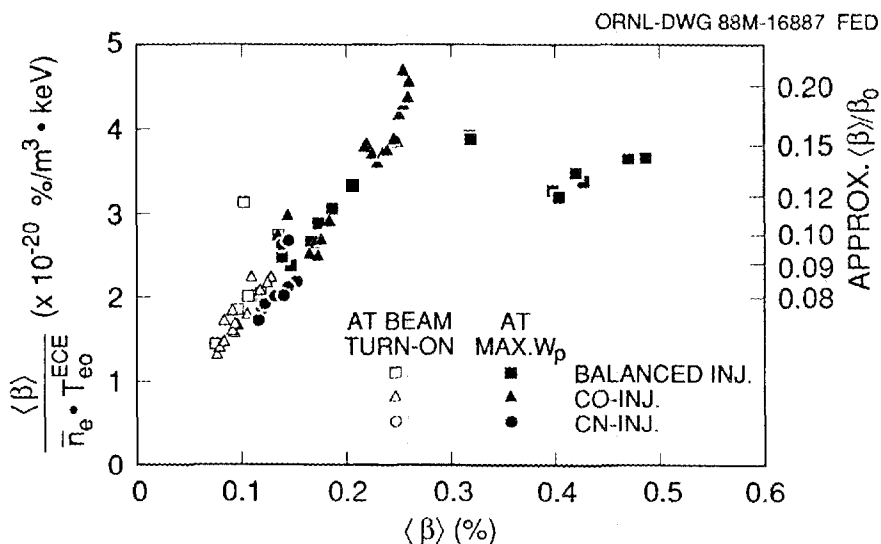


Fig. 6. Pressure “broadness” parameter ($\propto \langle\beta\rangle/\beta_0$) versus volume-average beta.

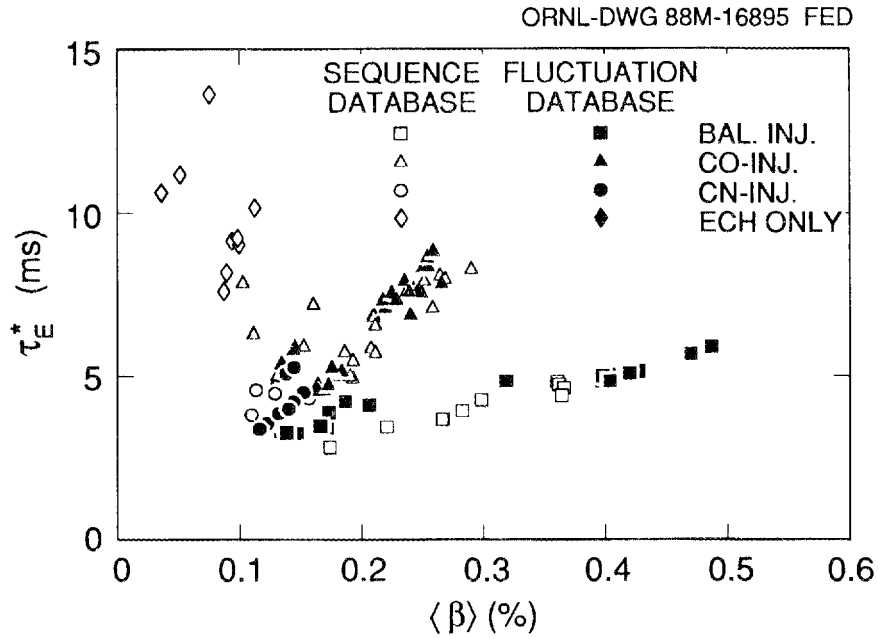


Fig. 7. Global energy confinement time versus volume-average beta.

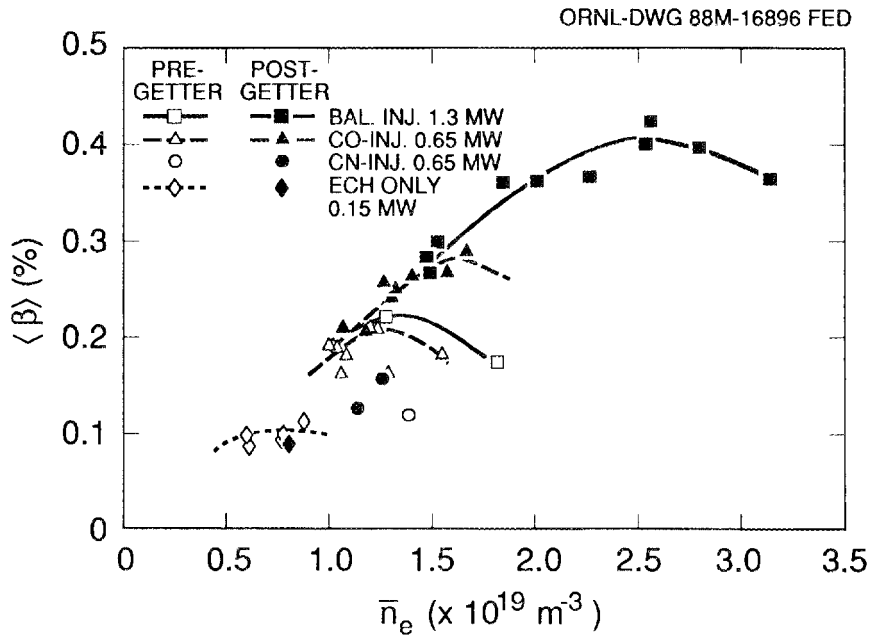


Fig. 8. Volume-average beta versus line-average electron density.

The saturation threshold increases with increasing heating power and improving cleanliness. This translates into an empirical scaling law,

$$\tau_E^* \propto P_{\text{abs}}^{-0.65} \bar{n}_e^{+0.57} ,$$

implying that confinement deterioration is offset by the favorable \bar{n}_e (or beta) dependence.

More comprehensive studies in the future will be aimed at correlations of transport, beta, and fluctuations. These studies will use configuration control (with vertical fields), profile variations (with limiter, intentional field errors, and pellet injection), and internal fluctuation diagnostics (reciprocating Langmuir probe, microwave reflectometer, and heavy ion beam probe).

ACKNOWLEDGMENT

We acknowledge with appreciation the contributions of our many colleagues in the ATF Group.

REFERENCES

- [1] J. F. Lyon et al., "The Advanced Toroidal Facility," *Fusion Technol.* **10**, 179 (1986).
- [2] M. J. Saltmarsh et al., "Initial Experimental Results from the ATF Torsatron," in *Plasma Physics and Controlled Nuclear Fusion Research (Proc. 12th Int. Conf. Nice, 1988)* IAEA, Vienna (in press, 1989).
- [3] R. J. Colchin et al., "Correction of Field Errors in the ATF Torsatron," paper P2B10 presented at the 16th European Conference on Controlled Fusion and Plasma Physics, Venice, March 13–17, 1989 (to be published in the proceedings).
- [4] P. K. Mioduszewski et al., "Edge Plasma and Divertor Studies in the ATF Torsatron," paper P8B2 presented at the 16th European Conference on Controlled Fusion and Plasma Physics, Venice, March 13–17, 1989 (to be published in the proceedings).
- [5] R. C. Isler et al., "Impurity Studies in the Advanced Toroidal Facility," paper P8B1 presented at the 16th European Conference on Controlled Fusion and Plasma Physics, Venice, March 13–17, 1989 (to be published in the proceedings).
- [6] H. C. Howe et al., "Transport Modeling of ECH and Neutral-Beam-Heated Plasmas in the Advanced Toroidal Facility," paper P9B4 presented at the 16th European Conference on Controlled Fusion and Plasma Physics, Venice, March 13–17, 1989 (to be published in the proceedings).
- [7] B. A. Carreras et al., *A First Glance at the Initial ATF Experimental Results*, ORNL/TM-11102, Martin Marietta Energy Systems, Inc., Oak Ridge Natl. Lab., 1989.
- [8] B. A. Carreras, "Anomalous Transport in the Second Stability Regime," *Comments Plasma Phys. Controlled Fusion* **12**, 35 (1988).
- [9] J. H. Harris et al., "Fluctuation Studies for ATF," *Bull. Am. Phys. Soc.* **33**, 2070 (1988).

INTERNAL DISTRIBUTION

- | | | | |
|--------|-----------------|--------|---|
| 1. | G. L. Bell | 29. | J. S. Lyon |
| 2. | J. D. Bell | 30. | M. M. Menon |
| 3. | L. A. Berry | 31. | R. N. Morris |
| 4. | T. S. Bigelow | 32-36. | M. Murakami |
| 5-9. | B. A. Carreras | 37. | R. N. Morris |
| 10. | R. J. Colchin | 38. | G. H. Neilson |
| 11. | E. C. Crume | 39. | V. K. Paré |
| 12. | N. Dominguez | 40. | D. A. Rasmussen |
| 13. | R. A. Dory | 41. | T. E. Shannon |
| 14. | J. L. Dunlap | 42. | J. Sheffield |
| 15. | A. C. England | 43. | J. B. Wilgen |
| 16. | J. C. Glowienka | 44. | W. R. Wing |
| 17. | H. H. Haselton | 45-46. | Laboratory Records Department |
| 18-22. | J. H. Harris | 47. | Laboratory Records, ORNL-RC |
| 23. | L. D. Horton | 48-49. | Central Research Library |
| 24. | H. C. Howe | 50. | Document Reference Section |
| 25. | R. C. Isler | 51. | Fusion Energy Division Library |
| 25. | T. C. Jernigan | 52. | Fusion Energy Division
Publications Office |
| 26. | J. N. Leboeuf | 53. | ORNL Patent Office |
| 27. | M. S. Lubell | | |
| 28. | V. E. Lynch | | |

EXTERNAL DISTRIBUTION

54. F. S. B. Anderson, University of Wisconsin, Madison, WI 53706
55. H. Kaneko, Plasma Physics Laboratory, Kyoto University, Gokasho, Uji, Kyoto, Japan
56. R. R. Kindsfather, IGEN, Inc., 1530 East Jefferson Street, Rockville, MD 20852
57. Office of the Assistant Manager for Energy Research and Development, U.S. Department of Energy, Oak Ridge Operations Office, P. O. Box E, Oak Ridge, TN 37831
58. J. D. Callen, Department of Nuclear Engineering, University of Wisconsin, Madison, WI 53706-1687
59. J. F. Clarke, Director, Office of Fusion Energy, Office of Energy Research, ER-50 Germantown, U.S. Department of Energy, Washington, DC 20545

60. R. W. Conn, Department of Chemical, Nuclear, and Thermal Engineering, University of California, Los Angeles, CA 90024
61. S. O. Dean, Fusion Power Associates, Inc., 2 Professional Drive, Suite 248, Gaithersburg, MD 20879
62. H. K. Forsen, Bechtel Group, Inc., Research Engineering, P. O. Box 3965, San Francisco, CA 94119
63. J. R. Gilleland, L-644, Lawrence Livermore National Laboratory, P.O. Box 5511, Livermore, CA 94550
64. R. W. Gould, Department of Applied Physics, California Institute of Technology, Pasadena, CA 91125
65. R. A. Gross, Plasma Research Laboratory, Columbia University, New York, NY 10027
66. D. M. Meade, Princeton Plasma Physics Laboratory, P.O. Box 451, Princeton, NJ 08543
67. M. Roberts, International Programs, Office of Fusion Energy, Office of Energy Research, ER-52 Germantown, U.S. Department of Energy, Washington, DC 20545
68. W. M. Stacey, School of Nuclear Engineering and Health Physics, Georgia Institute of Technology, Atlanta, GA 30332
69. D. Steiner, Nuclear Engineering Department, NES Building, Tibbetts Avenue, Rensselaer Polytechnic Institute, Troy, NY 12181
70. R. Varma, Physical Research Laboratory, Navrangpura, Ahmedabad 380009, India
71. Bibliothek, Max-Planck Institut für Plasmaphysik, Boltzmannstrasse 2, D-8046 Garching, Federal Republic of Germany
72. Bibliothek, Institut für Plasmaphysik, KFA Jülich GmbH, Postfach 1913, D-5170 Jülich, Federal Republic of Germany
73. Bibliothek, KfK Karlsruhe GmbH, Postfach 3640, D-7500 Karlsruhe 1, Federal Republic of Germany
74. Bibliotheque, Centre de Recherches en Physique des Plasmas, Ecole Polytechnique Fédérale de Lausanne, 21 Avenue des Bains, CH-1007 Lausanne, Switzerland
75. R. Aymar, CEN/Cadarache, Departement de Recherches sur la Fusion Contrôlée, F-13108 Saint-Paul-lez-Durance Cedex, France
76. Bibliothèque, CEN/Cadarache, F-13108 Saint-Paul-lez-Durance Cedex, France
77. Library, Culham Laboratory, UKAEA, Abingdon, Oxfordshire, OX14 3DB, England
78. Library, JET Joint Undertaking, Abingdon, Oxfordshire OX14 3EA, England
79. Library, FOM-Instituut voor Plasmafysica, Rijnhuizen, Edisonbaan 14, 3439 MN Nieuwegein, The Netherlands
80. Library, Institute of Plasma Physics, Nagoya University, Chikusa-ku, Nagoya 464, Japan

81. Library, International Centre for Theoretical Physics, P.O. Box 586, I-34100 Trieste, Italy
82. Library, Centro Recherche Energia Frascati, C.P. 65, I-00044 Frascati (Roma), Italy
83. Library, Plasma Physics Laboratory, Kyoto University, Gokasho, Uji, Kyoto 611, Japan
84. Plasma Research Laboratory, Australian National University, P.O. Box 4, Canberra, A.C.T. 2601, Australia
85. Library, Japan Atomic Energy Research Institute, Naka Fusion Research Establishment, 801-1 Mukoyama, Naka-machi, Naka-gun, Ibaraki-ken, Japan
86. G. A. Eliseev, I. V. Kurchatov Institute of Atomic Energy, P. O. Box 3402, 123182 Moscow, U.S.S.R.
87. V. A. Glukhikh, Scientific-Research Institute of Electro-Physical Apparatus, 188631 Leningrad, U.S.S.R.
88. I. Shpigel, Institute of General Physics, U.S.S.R. Academy of Sciences, Ulitsa Vavilova 38, Moscow, U.S.S.R.
89. D. D. Ryutov, Institute of Nuclear Physics, Siberian Branch of the Academy of Sciences of the U.S.S.R., Sovetskaya St. 5, 630090 Novosibirsk, U.S.S.R.
90. V. T. Tolok, Kharkov Physical-Technical Institute, Academical St. 1, 310108 Kharkov, U.S.S.R.
91. Deputy Director, Southwestern Institute of Physics, P.O. Box 15, Leshan, Sichuan, China (PRC)
92. Director, The Institute of Plasma Physics, P.O. Box 26, Hefei, Anhui, China (PRC)
93. R. A. Blanken, Experimental Plasma Research Branch, Division of Applied Plasma Physics, Office of Fusion Energy, Office of Energy Research, ER-542, Germantown, U.S. Department of Energy, Washington, DC 20545
94. K. Bol, Princeton Plasma Physics Laboratory, P.O. Box 451, Princeton, NJ 08543
95. R. A. E. Bolton, IREQ Hydro-Quebec Research Institute, 1800 Montee Ste.-Julie, Varennes, P.Q. JOL 2P0, Canada
96. D. H. Crandall, Experimental Plasma Research Branch, Division of Applied Plasma Physics, Office of Fusion Energy, Office of Energy Research, ER-542, Germantown, U.S. Department of Energy, Washington, DC 20545
97. R. L. Freeman, General Atomics, P.O. Box 85608, San Diego, CA 92138-5608
98. K. W. Gentle, RLM 11.222, Institute for Fusion Studies, University of Texas, Austin, TX 78712
99. R. J. Goldston, Princeton Plasma Physics Laboratory, P.O. Box 451, Princeton, NJ 08543
100. J. C. Hosea, Princeton Plasma Physics Laboratory, P.O. Box 451, Princeton, NJ 08543

101. D. Markevich, Division of Confinement Systems, Office of Fusion Energy, Office of Energy Research, ER-55, Germantown, U.S. Department of Energy, Washington, DC 20545
102. R. H. McKnight, Experimental Plasma Research Branch, Division of Applied Plasma Physics, Office of Fusion Energy, Office of Energy Research, ER-542, Germantown, U.S. Department of Energy, Washington, DC 20545
103. E. Oktay, Division of Confinement Systems, Office of Fusion Energy, Office of Energy Research, ER-55, Germantown, U.S. Department of Energy, Washington, DC 20545
104. D. Overskei, General Atomics, P.O. Box 85608, San Diego, CA 92138-5608
105. R. R. Parker, Plasma Fusion Center, NW 16-288, Massachusetts Institute of Technology, Cambridge, MA 02139
106. W. L. Sadowski, Fusion Theory and Computer Services Branch, Division of Applied Plasma Physics, Office of Fusion Energy, Office of Energy Research, ER-541, Germantown, U.S. Department of Energy, Washington, DC 20545
107. J. W. Willis, Division of Confinement Systems, Office of Fusion Energy, Office of Energy Research, ER-55, Germantown, U.S. Department of Energy, Washington, DC 20545
108. A. P. Navarro, Division de Fusion, CIEMAT, Avenida Complutense 22, E-28040 Madrid, Spain
109. Laboratory for Plasma and Fusion Studies, Department of Nuclear Engineering, Seoul National University, Shinrim-dong, Gwanak-ku, Seoul 151, Korea
110. J. L. Johnson, Plasma Physics Laboratory, Princeton University, P.O. Box 451, Princeton, NJ 08543
111. L. M. Kovrizhnykh, Institute of General Physics, U.S.S.R. Academy of Sciences, Ulitsa Vavilova 38, 117924 Moscow, U.S.S.R.
112. O. Motojima, Plasma Physics Laboratory, Kyoto University, Gokasho, Uji, Kyoto, Japan
113. V. D. Shafranov, I. V. Kurchatov Institute of Atomic Energy, P.O. Box 3402, 123182 Moscow, U.S.S.R.
114. J. L. Shohet, Torsatron/Stellarator Laboratory, University of Wisconsin, Madison, WI 53706
115. H. Wobig, Max-Planck Institut fur Plasmaphysik, D-8046 Garching, Federal Republic of Germany
- 116-166. Given distribution as shown in OSTI-4500, Magnetic Fusion Energy (Category Distribution UC-426, Experimental Plasma Physics)